

# Neutrino Oscillation Constraints on $U(1)'$ Models: from Non-Standard Interactions to Long-Range Forces

Pilar Coloma,<sup>a</sup> M. C. Gonzalez-Garcia,<sup>b,c,d</sup> Michele Maltoni<sup>a</sup>

<sup>a</sup>*Instituto de Física Teórica UAM/CSIC, Calle de Nicolás Cabrera 13–15, Universidad Autónoma de Madrid, Cantoblanco, E-28049 Madrid, Spain*

<sup>b</sup>*Departament de Física Quàntica i Astrofísica and Institut de Ciències del Cosmos, Universitat de Barcelona, Diagonal 647, E-08028 Barcelona, Spain*

<sup>d</sup>*Institució Catalana de Recerca i Estudis Avançats (ICREA), Pg. Lluís Companys 23, E-08010 Barcelona, Spain*

<sup>e</sup>*C.N. Yang Institute for Theoretical Physics, Stony Brook University, Stony Brook, NY 11794-3840, USA*

*E-mail:* [pilar.coloma@ift.csic.es](mailto:pilar.coloma@ift.csic.es),

[maria.gonzalez-garcia@stonybrook.edu](mailto:maria.gonzalez-garcia@stonybrook.edu), [michele.maltoni@csic.es](mailto:michele.maltoni@csic.es)

**ABSTRACT:** We quantify the effect of gauge bosons from a weakly coupled lepton flavor dependent  $U(1)'$  interaction on the matter background in the evolution of solar, atmospheric, reactor and long-baseline accelerator neutrinos in the global analysis of oscillation data. The analysis is performed for interaction lengths ranging from the Sun-Earth distance to effective contact neutrino interactions. We survey  $\sim 10000$  set of models characterized by the six relevant fermion  $U(1)'$  charges and find that in all cases, constraints on the coupling and mass of the  $Z'$  can be derived. We also find that about 5% of the  $U(1)'$  model charges lead to a viable LMA-D solution but this is only possible in the contact interaction limit. We explicitly quantify the constraints for a variety of models including  $U(1)_{B-3L_e}$ ,  $U(1)_{B-3L_\mu}$ ,  $U(1)_{B-3L_\tau}$ ,  $U(1)_{B-\frac{3}{2}(L_\mu+L_\tau)}$ ,  $U(1)_{L_e-L_\mu}$ ,  $U(1)_{L_e-L_\tau}$ ,  $U(1)_{L_e-\frac{1}{2}(L_\mu+L_\tau)}$ . We compare the constraints imposed by our oscillation analysis with the strongest bounds from fifth force searches, violation of equivalence principle as well as bounds from scattering experiments and white dwarf cooling. Our results show that generically, the oscillation analysis improves over the existing bounds from gravity tests for  $Z'$  lighter than  $\sim 10^{-8} \rightarrow 10^{-11}$  eV depending on the specific couplings. In the contact interaction limit, we find that for most models listed above there are values of  $g'$  and  $M_{Z'}$  for which the oscillation analysis provides constraints beyond those imposed by laboratory experiments. Finally we illustrate the range of  $Z'$  and couplings leading to a viable LMA-D solution for two sets of models.

**KEYWORDS:** neutrino physics, solar and atmospheric neutrinos

---

## Contents

<b>1</b>	<b>Introduction</b>	<b>1</b>
<b>2</b>	<b>Formalism</b>	<b>3</b>
2.1	The large ( $M_{Z'} \gtrsim 10^{-12}$ eV) $M_{Z'}$ limit: the NSI regime	5
2.2	The finite $M_{Z'}$ case: the long-range interaction regime	8
<b>3</b>	<b>Results of the global oscillation analysis</b>	<b>9</b>
3.1	Bounds	11
3.2	Models for LMA-D	15
<b>4</b>	<b>Conclusions</b>	<b>18</b>
<b>A</b>	<b>Bounds from non-oscillation experiments</b>	<b>19</b>

---

## 1 Introduction

Experiments measuring the flavor composition of neutrinos produced in the Sun, in the Earth’s atmosphere, in nuclear reactors and in particle accelerators have established that lepton flavor is not conserved in neutrino propagation, but it oscillates with a wavelength which depends on distance and energy. This demonstrates beyond doubt that neutrinos are massive and that the mass states are non-trivial admixtures of flavor states [1, 2], see Ref. [3] for an overview.

When traveling through matter, the flavor evolution of the neutrino ensemble is affected by the difference in the effective potential induced by elastic forward scattering of neutrino with matter, the so-called Mikheev-Smirnov-Wolfenstein (MSW) mechanism [4, 5]. Within the context of the Standard Model (SM) of particle interactions, this effect is fully determined and leads to a matter potential which, for neutral matter, is proportional to the number density of electrons at the neutrino position,  $V = \sqrt{2}G_F N_e(r)$ , and which only affects electron neutrinos. New flavor dependent interactions can modify the matter potential and consequently alter the pattern of flavor transitions, thus leaving imprints in the oscillation data involving neutrinos which have traveled through large regions of matter, as is the case for solar and atmospheric neutrinos.

Forward elastic scattering takes place in the limit of zero momentum transfer, so as long as the range of the interaction is shorter than the scale over which the matter density extends, the effective matter potential can be obtained in the contact interaction approximation between the neutrinos and the matter particles. The paradigmatic example is

provided by neutral current non-standard interactions (NSI) [4, 6, 7] between neutrinos and matter (for recent reviews, see [8–11]), which can be parametrized as

$$\mathcal{L}_{\text{NSI}} = -2\sqrt{2}G_F \sum_{f,P,\alpha,\beta} \varepsilon_{\alpha\beta}^{f,P} (\bar{\nu}_\alpha \gamma^\mu P_L \nu_\beta) (\bar{f} \gamma_\mu P f), \quad (1.1)$$

where  $G_F$  is the Fermi constant,  $\alpha, \beta$  are flavor indices,  $P \equiv P_L, P_R$  and  $f$  is a SM charged fermion. These operators are expected to arise generically from the exchange of some mediator state heavy enough for the contact interaction approximation to hold. In this notation,  $\varepsilon_{\alpha\beta}^{f,P}$  parametrizes the strength of the new interaction with respect to the Fermi constant,  $\varepsilon_{\alpha\beta}^{f,P} \sim \mathcal{O}(G_X/G_F)$ . Generically they modify the matter potential in neutrino propagation, but – being local interactions – the resulting potential is still proportional to the number density of particles in the medium at the neutrino position. Since such modifications arise from a coherent effect, oscillation bounds apply even to NSI induced by ultra light mediators, as long as their interaction length is shorter than the neutrino oscillation length. For the experiments considered here, such condition is fulfilled as long as  $M_{Z'} \gtrsim 10^{-12}$  eV [12].

Conversely, if the mediator is too light then the contact interaction approximation is no longer valid, and the flavor dependent forces between neutrino and matter particles become long-range. In this case neutrino propagation can still be described in terms of a matter potential, which however is no longer simply determined by the number density of particles in the medium at the neutrino position, but it depends instead on the average of the matter density within a radius  $\sim 1/M_{Z'}$  around it [12–16].

At present, the global analysis of data from oscillation experiments provides some of the strongest constraints on the size of the NSI affecting neutrino propagation [17–19]. Analysis of early oscillation data was also used to impose constraints on flavor dependent long-range forces [12–14].

Straightforward constructions leading to Eq. (1.1) have an extended gauge sector with an additional  $U(1)'$  symmetry with charge involving some of the lepton flavors and an heavy enough gauge boson. Conversely if the gauge boson is light enough a long range force will be generated. Thus the analysis of neutrino oscillation data can shed light on the valid range of  $Z'$  mass and coupling in both regimes. Following this approach, the marginalized bounds on the NSI coefficients derived from the global analysis of oscillations in presence of NSI performed in Ref. [19] were adapted to place constraints on the coupling and mass of the new gauge boson both in the NSI limit [20] and in the long-range regime [16] for several  $U(1)'$  flavor symmetries. However, strictly speaking, the bounds derived in Ref. [19] cannot be directly used to constraint the  $U(1)'$  scenarios because in the latter case only flavor diagonal interactions (and only some of them depending on the  $U(1)'$  charge) are generated, while the bounds derived in Ref. [19] were obtained in the most general parameter space with all relevant four-fermion interactions (flavor conserving and flavor changing) being simultaneously non-vanishing. In order to derive statistically consistent bounds on each  $U(1)'$  scenario a dedicated analysis has to be performed in its reduced parameter space.

With this motivation, in this work we perform such dedicated global analysis of oscillation data in the framework of lepton flavor dependent  $U(1)'$  interactions which affect

the neutrino evolution in matter, with interaction lengths ranging from the Sun-Earth distance to effective contact neutrino interactions. In Sec. 2 we describe the models which will be studied and derive the matter potential generated both in the contact interaction limit (in Sec. 2.1) and in the case of finite interaction range (in Sec. 2.2) as a function of the  $U(1)'$  charges. The results of the global analysis are presented in Sec. 3. In particular the bounds imposed by the analysis and how they compare with those from other experiments are presented in Sec. 3.1. An additional consideration that we take into account is that in the presence of NSI a degeneracy exists in oscillation data, leading to the so called LMA-Dark (LMA-D) [21] solution first observed in solar neutrinos, where for suitable NSI the data can be explained by a mixing angle  $\theta_{12}$  in the second octant. For this new solution to appear the new interactions must be such that the matter potential difference for electron neutrinos reverses its sign with respect to that in the SM. It is not trivial to generate such large effects without conflicting with bounds from other experiments, though models with light mediators (*i.e.*, below the electroweak scale) have been proposed as viable candidates [9, 10, 22–25]. Section 3.2 contains our findings on viable models for LMA-D. We summarize our conclusions in Sec. 4. We present some details of the translation of the bounds from some experiments to the models studied in an appendix.

## 2 Formalism

We are going to focus on  $U(1)'$  models which can be tested in neutrino oscillation experiments via its contribution to the matter potential. As a start this requires that the new gauge boson couples to the fermions of the first generation.

An important issue when enlarging the Standard Model with a new  $U(1)'$  gauge group is the possibility of mixing between the three neutral gauge bosons of the model which can, in general, be induced in either kinetic or mass terms. While kinetic mixing is fairly generic as it can be generated at the loop level with the SM particle contents, matter mixing is model dependent as it requires an extended scalar sector with a vacuum expectation value charged both under the SM and the  $U(1)'$ . In what respects the effect of the new  $U(1)'$  in oscillation experiments an important observation is that if the new interaction does not couple directly to fermions of the first generation, no matter effects can be generated by kinetic mixing [20]. Thus neglecting mixing effects yields the most model independent and conservative bounds from neutrino oscillation results. So in what follows we are going to work under the assumption that the  $Z'$  mixing with SM gauge bosons can be safely neglected.

In addition we notice that only vector interactions contribute to the matter potential in neutrino propagation. Altogether the part of the  $U(1)'$  Lagrangian relevant for propagation in ordinary matter has the most general form

$$\begin{aligned} \mathcal{L}_{Z'}^{\text{matter}} = & -g' (a_u \bar{u} \gamma^\alpha u + a_d \bar{d} \gamma^\alpha d + a_e \bar{e} \gamma^\alpha e \\ & + b_e \bar{\nu}_e \gamma^\alpha P_L \nu_e + b_\mu \bar{\nu}_\mu \gamma^\alpha P_L \nu_\mu + b_\tau \bar{\nu}_\tau \gamma^\alpha P_L \nu_\tau) Z'_\alpha \end{aligned} \quad (2.1)$$

with arbitrary charges  $a_{u,d,e}$  and  $b_{e,\mu,\tau}$ .

Model	$a_u$	$a_d$	$a_e$	$b_e$	$b_\mu$	$b_\tau$
$B - 3L_e$	$\frac{1}{3}$	$\frac{1}{3}$	$-3$	$-3$	$0$	$0$
$B - 3L_\mu$	$\frac{1}{3}$	$\frac{1}{3}$	$0$	$0$	$-3$	$0$
$B - 3L_\tau$	$\frac{1}{3}$	$\frac{1}{3}$	$0$	$0$	$0$	$-3$
$B - \frac{3}{2}(L_\mu + L_\tau)$	$\frac{1}{3}$	$\frac{1}{3}$	$0$	$0$	$-\frac{3}{2}$	$-\frac{3}{2}$
$L_e - L_\mu$	$0$	$0$	$1$	$1$	$-1$	$0$
$L_e - L_\tau$	$0$	$0$	$1$	$1$	$0$	$-1$
$L_e - \frac{1}{2}(L_\mu + L_\tau)$	$0$	$0$	$1$	$1$	$-\frac{1}{2}$	$-\frac{1}{2}$
Ref. [22]	$\frac{1}{3}$	$\frac{1}{3}$	$0$	$0$	$1$	$1$
$L_e + 2L_\mu + 2L_\tau$	$0$	$0$	$1$	$1$	$2$	$2$

**Table 1.** Relevant charges for the matter effects in neutrino oscillation experiments corresponding to a selection of models studied in the literature.

These charges can be accommodated in generalized anomaly free UV-complete models including only the SM particles plus right-handed neutrinos [26]. If, in addition, one requires all couplings to be vector-like and the quark couplings to be generation independent, the condition of anomaly cancellation for models with only SM plus right handed neutrinos imposes constraints over the six charges above and one ends with a subclass of models characterized by three independent charges which can be chosen to be, for example,  $B - L$ ,  $(L_\mu - L_\tau)$ , and  $(L_\mu - L_e)$  [20]:

$$c_{\text{BL}}(B - L) + c_{\mu\tau}(L_\mu - L_\tau) + c_{\mu e}(L_\mu - L_e), \quad (2.2)$$

so  $a_u = a_d = c_{\text{BL}}/3$ ,  $a_e = b_e = -(c_{\text{BL}} + c_{\mu e})$ ,  $b_\mu = -c_{\text{BL}} + c_{\mu e} + c_{\mu\tau}$ , and  $b_\tau = -(c_{\text{BL}} + c_{\mu\tau})$ . For convenience, in table 1 we list the charges corresponding to some of the models discussed in the literature.

In general, the evolution of the neutrino and antineutrino flavor state during propagation is governed by the Hamiltonian:

$$H^\nu = H_{\text{vac}} + H_{\text{mat}} \quad \text{and} \quad H^{\bar{\nu}} = (H_{\text{vac}} - H_{\text{mat}})^*, \quad (2.3)$$

where  $H_{\text{vac}}$  is the vacuum part which in the flavor basis  $(\nu_e, \nu_\mu, \nu_\tau)$  reads

$$H_{\text{vac}} = U_{\text{vac}} D_{\text{vac}} U_{\text{vac}}^\dagger \quad \text{with} \quad D_{\text{vac}} = \frac{1}{2E_\nu} \text{diag}(0, \Delta m_{21}^2, \Delta m_{31}^2). \quad (2.4)$$

Here  $U_{\text{vac}}$  denotes the three-lepton mixing matrix in vacuum [1, 27, 28]. Following the convention of Ref. [29], we define  $U_{\text{vac}} = R_{23}(\theta_{23})R_{13}(\theta_{13})\tilde{R}_{12}(\theta_{12}, \delta_{\text{CP}})$ , where  $R_{ij}(\theta_{ij})$  is a rotation of angle  $\theta_{ij}$  in the  $ij$  plane and  $\tilde{R}_{12}(\theta_{12}, \delta_{\text{CP}})$  is a complex rotation by angle  $\theta_{12}$  and phase  $\delta_{\text{CP}}$ .

Concerning the matter part  $H_{\text{mat}}$  of the Hamiltonian generated by the SM together with the  $U(1)'$  interactions in (2.1), its form depends on the new interaction length determined by the  $Z'$  mass as we discuss next.

## 2.1 The large ( $M_{Z'} \gtrsim 10^{-12}$ eV) $M_{Z'}$ limit: the NSI regime

In the limit of large  $M_{Z'}$ , the  $Z'$  field can be integrated out from the spectrum and Eq. (2.1) generate effective dimension-six four-fermion interactions leading to Neutral Current NSI between neutrinos and matter which are usually parametrized in the form of Eq. (1.1). The coefficients  $\varepsilon_{\alpha\beta}^{f,P}$  parametrizes the strength of the new interaction with respect to the Fermi constant, with

$$\varepsilon_{\alpha\beta}^{f,L} = \varepsilon_{\alpha\beta}^{f,R} = \delta_{\alpha\beta} \frac{1}{2\sqrt{2}G_F} \frac{g'^2}{M_{Z'}^2} a_f b_\alpha \equiv \delta_{\alpha\beta} \frac{1}{2} a_f b_\alpha \varepsilon^0 \quad (2.5)$$

where we have introduced the notation

$$\varepsilon^0 \equiv \frac{1}{\sqrt{2}G_F} \frac{g'^2}{M_{Z'}^2} \quad (2.6)$$

As it is well known, only vector NSI contribute to the matter potential in neutrino oscillations. It is therefore convenient to define the parameters relevant for neutrino oscillation experiments as:

$$\varepsilon_{\alpha\beta}^f \equiv \varepsilon_{\alpha\beta}^{f,L} + \varepsilon_{\alpha\beta}^{f,R} = \delta_{\alpha\beta} a_f b_\alpha \varepsilon^0. \quad (2.7)$$

These interactions lead to a flavour diagonal modification of the matter potential

$$H_{\text{mat}} = \sqrt{2}G_F N_e(\vec{x}) \begin{pmatrix} 1 + \mathcal{E}_{ee}(\vec{x}) & 0 & 0 \\ 0 & \mathcal{E}_{\mu\mu}(\vec{x}) & 0 \\ 0 & 0 & \mathcal{E}_{\tau\tau}(\vec{x}) \end{pmatrix} \quad (2.8)$$

where the “+1” term in the  $ee$  entry accounts for the standard contribution, and

$$\mathcal{E}_{\alpha\alpha}(\vec{x}) = \sum_{f=e,u,d} \frac{N_f(\vec{x})}{N_e(\vec{x})} \varepsilon_{\alpha\alpha}^f \quad (2.9)$$

describes the non-standard part. Here  $N_f(\vec{x})$  is the number density of fermion  $f$  at the position  $\vec{x}$  along the neutrino trajectory. In Eq. (2.9) we have limited the sum to the charged fermions present in ordinary matter,  $f = e, u, d$ . Taking into account that  $N_u(\vec{x}) = 2N_p(\vec{x}) + N_n(\vec{x})$  and  $N_d(\vec{x}) = N_p(\vec{x}) + 2N_n(\vec{x})$ , and also that matter neutrality implies  $N_p(\vec{x}) = N_e(\vec{x})$ , Eq. (2.9) becomes:

$$\mathcal{E}_{\alpha\alpha}(\vec{x}) = (\varepsilon_{\alpha\alpha}^e + \varepsilon_{\alpha\alpha}^p) + Y_n(\vec{x}) \varepsilon_{\alpha\alpha}^n \quad \text{with} \quad Y_n(\vec{x}) \equiv \frac{N_n(\vec{x})}{N_e(\vec{x})} \quad (2.10)$$

where

$$\varepsilon_{\alpha\alpha}^p \equiv 2\varepsilon_{\alpha\alpha}^u + \varepsilon_{\alpha\alpha}^d = a_p b_\alpha \varepsilon^0, \quad \varepsilon_{\alpha\alpha}^n \equiv 2\varepsilon_{\alpha\alpha}^d + \varepsilon_{\alpha\alpha}^u = a_n b_\alpha \varepsilon^0. \quad (2.11)$$

and we have introduced the proton and neutron  $Z'$  couplings

$$a_p \equiv 2a_u + a_d, \quad a_n \equiv 2a_d + a_u. \quad (2.12)$$

As discussed in Ref. [17], in the Earth the neutron/proton ratio  $Y_n(\vec{x})$  which characterize the matter chemical composition can be taken to be constant to very good approximation. The PREM model [30] fixes  $Y_n = 1.012$  in the Mantle and  $Y_n = 1.137$  in the Core, with an

average value  $Y_n^\oplus = 1.051$  all over the Earth. Setting therefore  $Y_n(\vec{x}) \equiv Y_n^\oplus$  in Eqs. (2.9) and (2.10) we get  $\mathcal{E}_{\alpha\alpha}(\vec{x}) \equiv \varepsilon_{\alpha\alpha}^\oplus$  with:

$$\begin{aligned}\varepsilon_{\alpha\alpha}^\oplus &= \varepsilon_{\alpha\alpha}^e + (2 + Y_n^\oplus) \varepsilon_{\alpha\alpha}^u + (1 + 2Y_n^\oplus) \varepsilon_{\alpha\alpha}^d = (\varepsilon_{\alpha\alpha}^e + \varepsilon_{\alpha\alpha}^p) + Y_n^\oplus \varepsilon_{\alpha\alpha}^n \\ &= [(a_e + a_p) + Y_n^\oplus a_n] b_\alpha \varepsilon^0.\end{aligned}\quad (2.13)$$

For what concerns the study of propagation of solar and KamLAND neutrinos one can work in the one mass dominance approximation,  $\Delta m_{31}^2 \rightarrow \infty$  (which effectively means that  $G_F N_e(\vec{x}) \mathcal{E}_{\alpha\alpha}(\vec{x}) \ll \Delta m_{31}^2 / E_\nu$ ). In this approximation the survival probability  $P_{ee}$  can be written as [31, 32]

$$P_{ee} = c_{13}^4 P_{\text{eff}} + s_{13}^4 \quad (2.14)$$

The probability  $P_{\text{eff}}$  can be calculated in an effective  $2 \times 2$  model described by the Hamiltonian  $H_{\text{eff}} = H_{\text{vac}}^{\text{eff}} + H_{\text{mat,SM}}^{\text{eff}} + H_{\text{mat,Z'}}^{\text{eff}}$ , with:

$$H_{\text{vac}}^{\text{eff}} = \frac{\Delta m_{21}^2}{4E_\nu} \begin{pmatrix} -\cos 2\theta_{12} & \sin 2\theta_{12} e^{i\delta_{\text{CP}}} \\ \sin 2\theta_{12} e^{-i\delta_{\text{CP}}} & \cos 2\theta_{12} \end{pmatrix}, \quad (2.15)$$

$$H_{\text{mat,SM}}^{\text{eff}} = \sqrt{2} G_F N_e(\vec{x}) \begin{pmatrix} c_{13}^2 & 0 \\ 0 & 0 \end{pmatrix} \quad (2.16)$$

and

$$H_{\text{mat,Z'}}^{\text{eff}} = \sqrt{2} G_F N_e(\vec{x}) \varepsilon^0 [a_e + a_p + Y_n(\vec{x}) a_n] \begin{pmatrix} -b_D & b_N \\ b_N & b_D \end{pmatrix} \quad (2.17)$$

where

$$b_D = -\frac{c_{13}^2}{2} (b_e - b_\mu) + \frac{s_{23}^2 - s_{13}^2 c_{23}^2}{2} (b_\tau - b_\mu), \quad (2.18)$$

$$b_N = s_{13} c_{23} s_{23} (b_\tau - b_\mu). \quad (2.19)$$

Following Ref. [19] we can rewrite the  $Z'$  contribution as:

$$H_{\text{mat,Z'}}^{\text{eff}} = \sqrt{2} G_F N_e(\vec{x}) [\cos \eta + Y_n(\vec{x}) \sin \eta] \begin{pmatrix} -\varepsilon_D^\eta & \varepsilon_N^\eta \\ \varepsilon_N^\eta & \varepsilon_D^\eta \end{pmatrix}, \quad (2.20)$$

where the angle  $\eta$  parametrizes the ratio of the charges of the matter particles as:

$$\cos \eta = \frac{a_e + a_p}{\sqrt{(a_e + a_p)^2 + a_n^2}}, \quad \sin \eta = \frac{a_n}{\sqrt{(a_e + a_p)^2 + a_n^2}}, \quad (2.21)$$

and

$$\varepsilon_{D,N}^\eta = \sqrt{(a_e + a_p)^2 + a_n^2} b_{D,N} \varepsilon^0. \quad (2.22)$$

The neutrino oscillation phenomenology in this regime reduces to a special subclass of the general NSI interactions analyzed in Ref. [19].<sup>1</sup> In particular, as a consequence of

---

<sup>1</sup>To be precise, the data analysis performed in Ref. [19] was restricted to NSI with quarks, ie  $a_e = 0$ . The formalism for matter effects can be trivially extended to NSI coupled to electrons as shown above. However, NSI coupled to electrons would affect not only neutrino propagation in matter as described, but also the neutrino-electron (ES) scattering cross-section in experiments such as SK, SNO and Borexino. In order to keep the analysis manageable, in Ref. [19], and in what follows, the NSI corrections to the ES scattering cross section in SK, SNO, and Borexino are neglected. In the absence of cancellations between propagation and interaction effects this renders the results of the oscillation analysis conservative.

the CPT symmetry (see also Refs. [17, 18, 29] for a discussion in the context of NSI) the neutrino evolution is invariant if the relevant Hamiltonian is transformed as  $H \rightarrow -H^*$ . In vacuum this transformation can be realized by changing the oscillation parameters as

$$\begin{aligned}\Delta m_{31}^2 &\rightarrow -\Delta m_{31}^2 + \Delta m_{21}^2 = -\Delta m_{32}^2, \\ \theta_{12} &\rightarrow \pi - \theta_{12}, \\ \delta_{\text{CP}} &\rightarrow \pi - \delta_{\text{CP}},\end{aligned}\tag{2.23}$$

where  $\delta_{\text{CP}}$  is the leptonic Dirac CP phase, and we are using here the parameterization conventions from Refs. [19, 29]. The symmetry is broken by the standard matter effect, which allows a determination of the octant of  $\theta_{12}$  and (in principle) of the sign of  $\Delta m_{31}^2$ . However, in the presence of the  $Z'$ -induced NSI, the symmetry can be restored if in addition to the transformation Eq. (2.23), the  $\mathcal{E}_{\alpha\alpha}(\vec{x})$  terms can be transformed as [18, 29, 33]

$$\begin{aligned}[\mathcal{E}_{ee}(\vec{x}) - \mathcal{E}_{\mu\mu}(\vec{x})] &\rightarrow -[\mathcal{E}_{ee}(\vec{x}) - \mathcal{E}_{\mu\mu}(\vec{x})] - 2, \\ [\mathcal{E}_{\tau\tau}(\vec{x}) - \mathcal{E}_{\mu\mu}(\vec{x})] &\rightarrow -[\mathcal{E}_{\tau\tau}(\vec{x}) - \mathcal{E}_{\mu\mu}(\vec{x})].\end{aligned}\tag{2.24}$$

Eq. (2.23) shows that this degeneracy implies a change in the octant of  $\theta_{12}$  (as manifest in the LMA-D fit to solar neutrino data [21]) as well as a change in the neutrino mass ordering, *i.e.*, the sign of  $\Delta m_{31}^2$ . For that reason it has been called “generalized mass ordering degeneracy” in Ref. [29]. Because of the position dependence of the NSI hamiltonian described by  $\mathcal{E}_{\alpha\alpha}(\vec{x})$  this degeneracy is only approximate, mostly due to the non-trivial neutron/proton ratio along the neutrino path inside the Sun. In what follows when marginalizing over  $\theta_{12}$  we consider two distinct parts of the parameter space: one with  $\theta_{12} < 45^\circ$ , which we denote as LIGHT, and one with  $\theta_{12} > 45^\circ$ , which we denote by DARK.

Apart from the appearance of this degenerate solution, another feature to consider in the global analysis of oscillation data in presence of NSI is the possibility to further improve the quality of the fit with respect to that of *standard*  $3\nu$  oscillations in the LIGHT sector. Till recently this was indeed the case because for the last decade the value of  $\Delta m_{21}^2$  preferred by KamLAND was somewhat higher than the one from solar experiments. This tension appeared due to a combination of two effects: the fact that the  $^8\text{B}$  measurements performed by SNO, SK and Borexino showed no evidence of the low energy spectrum turn-up expected in the standard LMA-MSW [4, 5] solution for the value of  $\Delta m_{21}^2$  favored by KamLAND, and the observation of a non-vanishing day-night asymmetry in SK, whose size was larger than the one predicted for the  $\Delta m_{21}^2$  value indicated by KamLAND. With the data included in the analysis in Ref. [19, 34] this resulted into a tension of  $\Delta\chi^2 \sim 7.4$  for the standard  $3\nu$  oscillations. Such tension could be alleviated in presence of a non-standard matter potential, thus leading to a possible decrease in the minimum  $\chi^2$ . However, with the latest 2970-days SK4 results presented at the Neutrino2020 conference [35] in the form of total energy spectrum and updated day-night asymmetry, the tension between the best fit  $\Delta m_{21}^2$  of KamLAND and that of the solar results has decreased. Currently they are compatible within  $1.1\sigma$  in the latest global analysis [36].



## 2.2 The finite $M_{Z'}$ case: the long-range interaction regime

If  $M_{Z'}$  is very light the four-fermion contact interaction approximation in Eq. (1.1) does not hold and the potential encountered by the neutrino in its trajectory depends on the integral of the source density within a radius  $\sim 1/M_{Z'}$  around it. However, following Ref. [12] the generalized matter potential can still be written as Eq. (2.8) provided that Eq. (2.9) is modified as:

$$\mathcal{E}_{\alpha\alpha}(\vec{x}) = \sum_{f=e,u,d} \frac{\hat{N}_f(\vec{x}, M_{Z'})}{N_e(\vec{x})} \varepsilon_{\alpha\alpha}^f \quad (2.25)$$

where

$$\hat{N}_f(\vec{x}, M_{Z'}) \equiv \frac{4\pi}{M_{Z'}^2} \int N_f(\vec{\rho}) \frac{e^{-M_{Z'}|\vec{\rho}-\vec{x}|}}{|\vec{\rho}-\vec{x}|} d^3\vec{\rho}. \quad (2.26)$$

Taking into account that ordinary matter is neutral and only contains  $f = e, u, d$ , we can rewrite Eq. (2.25) in a way that generalizes Eq. (2.10):

$$\begin{aligned} \mathcal{E}_{\alpha\alpha}(\vec{x}) &= F_e(\vec{x}, M_{Z'}) (\varepsilon_{\alpha\alpha}^e + \varepsilon_{\alpha\alpha}^p) + F_n(\vec{x}, M_{Z'}) Y_n(\vec{x}) \varepsilon_{\alpha\alpha}^n \\ \text{with } F_i(\vec{x}, M_{Z'}) &\equiv \frac{\hat{N}_i(\vec{x}, M_{Z'})}{N_i(\vec{x})} \quad \text{and } i \in \{e, n\}. \end{aligned} \quad (2.27)$$

For what concerns neutrinos traveling inside the Sun, the propagation effects induced by the new interactions are completely dominated by the solar matter distribution. Denoting by  $\vec{x}_\odot$  the center of the Sun and accounting for the spherical symmetry of the matter potential we can write:

$$\begin{aligned} F_i(\vec{x}, M_{Z'}) &\simeq F_i^\odot(|\vec{x} - \vec{x}_\odot|, M_{Z'}) \\ \text{with } F_i^\odot(r, M_{Z'}) &= \frac{1}{N_i^\odot(r)} \cdot \frac{M_{Z'}}{2r} \int_0^{R_\odot} \rho N_i^\odot(\rho) [e^{-M_{Z'}|\rho-r|} - e^{-M_{Z'}(\rho+r)}] d\rho. \end{aligned} \quad (2.28)$$

A similar formula can be derived for neutrinos traveling inside the Earth, but in this case the effective potential has an extra term induced by the Sun matter density. Concretely, denoting by  $\vec{x}_\oplus$  the center of the Earth and by  $X_\ominus = |\vec{x}_\odot - \vec{x}_\oplus|$  the Sun-Earth distance, we have:

$$\begin{aligned} F_i(\vec{x}, M_{Z'}) &\simeq F_i^\oplus(|\vec{x} - \vec{x}_\oplus|, M_{Z'}) \\ \text{with } F_i^\oplus(r, M_{Z'}) &= \frac{1}{N_i^\oplus(r)} M_{Z'} \left\{ \frac{1}{2r} \int_0^{R_\oplus} \rho N_i^\oplus(\rho) [e^{-M_{Z'}|\rho-r|} - e^{-M_{Z'}(\rho+r)}] d\rho \right. \\ &\quad \left. + \frac{e^{-M_{Z'}X_\ominus}}{X_\ominus} \int_0^{R_\odot} \rho N_i^\odot(\rho) \sinh(\rho M_{Z'}) d\rho \right\}. \end{aligned} \quad (2.29)$$

The solar-induced contribution becomes non-negligible when the range of the interactions,  $1/M_{Z'}$ , is comparable or larger than the Sun-Earth distance  $X_\ominus$ .

The factors  $F_i^\odot(r, M_{Z'})$  and  $F_i^\oplus(r, M_{Z'})$  represent the modification of the matter potential due to the finite range of the interaction mediated by the  $Z'$  with respect to that obtained in the contact interaction limit. Such limit is recovered when the range of the new

interactions become shorter than the typical size of the matter distribution, *i.e.*,  $R_{\odot(\oplus)}$ . Hence:

$$F_i^{\odot(\oplus)}(r, M_{Z'}) \rightarrow 1 \quad \text{for} \quad M_{Z'} \gg 1/R_{\odot(\oplus)}. \quad (2.30)$$

For solar neutrinos further simplification follows if one takes into account that for adiabatic transitions the dominant matter effects is generated by the potential at the neutrino production point which is close to the Sun center. So to a very good approximation one can scale the contact interaction potential with a position independent factor  $F_i^{\odot}(0, M_{Z'})$ . For the Earth matter potential the position dependence of the factor  $F_i^{\oplus}(r, M_{Z'})$  is very weak in the current experiments, so one can also scale the contact interaction potential with an approximate  $F_i^{\oplus}(\bar{r}, M_{Z'})$  evaluated at a fix  $\bar{r}$  which we take to be also  $\bar{r} = 0$ .

In Fig. 1 we plot these scale factors  $F_e^{\odot(\oplus)}(0, M_{Z'})$ . As seen in the figure for  $M_{Z'} \lesssim 10^{-13}$  eV the matter potential in the Earth is more suppressed with respect to that in the Sun. In principle, this opens the possibility of configurations for which the  $U(1)'$ -induced matter potential in the Sun is large enough without conflicting with bounds imposed by atmospheric and long-baseline experiments. This also implies that in the combined analysis of solar and KamLAND data, for a given value of  $M_{Z'}$ , the effective matter potential for solar neutrinos will be suppressed by a different factor than that for KamLAND antineutrinos. To illustrate the overall  $M_{Z'}$  dependence of the effect we show in Fig. 1 the effective suppression factor in the combined solar+KamLAND analysis calculated by scaling the results obtained for a specific model (concretely, for a  $Z'$  coupled to  $L_e - L_\mu$ , but the results are similar for models with other couplings) for each  $M_{Z'}$  to those obtained in the large  $M_{Z'}$  regime. As seen in the figure for  $M_{Z'} \gtrsim 10^{-10}$  eV both the effective potential in the Solar+KamLAND analysis and the Earth matter potential relevant for atmospheric and LBL neutrinos are well within the contact interaction regime. Conversely for  $M_{Z'} \lesssim 10^{-13}$  eV all the matter potentials in the analysis show deviations from the contact interaction regime.

Concerning the phenomenology of neutrino oscillations in the presence of the modified matter potential in this long-range interaction regime, the main difference with the NSI contact interaction case is the impossibility of realizing the “generalized mass ordering degeneracy” in Eqs. (2.23) and (2.24) because of the very different  $\vec{x}$  dependence of the SM matter potential and the one generated by the  $Z'$ . In other words, one cannot “flip the sign of the matter hamiltonian” by adding to the standard  $N_e(x)$  something which has a completely different  $\vec{x}$  profile. Hence, there is no LMA-D solution for these models. On the other hand, it is still possible, at least in principle, that a long-range potential leads to an improvement on the fit to solar and KamLAND data with respect to the pure LMA solution.

### 3 Results of the global oscillation analysis

We have performed a global fit to neutrino oscillation data in the framework of  $3\nu$  massive neutrinos with new neutrino-matter interactions generated by  $U(1)'$  models and characterized by the Lagrangian in Eq. (2.1). For the detailed description of methodology and data included we refer to the comprehensive global fit in Ref. [19] performed in the framework of

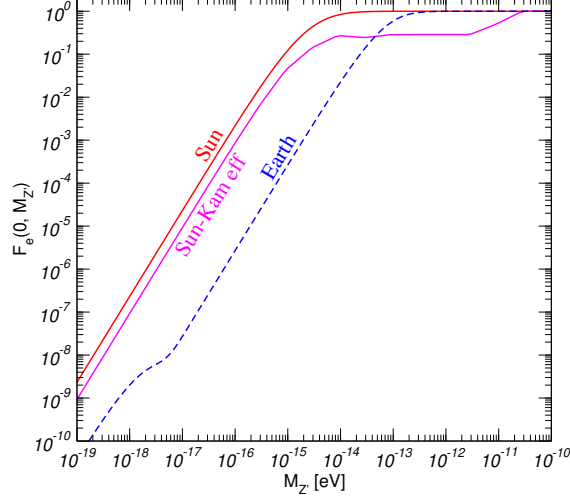


**Figure 1.** Effective suppression factor of the matter potential due to the long range of the  $U(1)'$  interactions as a function of  $M_{Z'}$ . The red (blue) curve corresponds to the potential in the Sun (Earth). The purple line corresponds to the effective combined suppression factor in the analysis of Solar+KamLAND data (see text for details).

three-flavor oscillations plus NSI. In addition in the present analysis we account for the latest LBL data samples included in NuFIT-5.0 [36] which includes the previously cited solar neutrinos 2970-days SK4 results [35], the updated medium baseline reactor samples from RENO [37] and Double Chooz [38], and the latest long-baseline samples from T2K [39] and NO $\nu$ A [40]. Notice that in order to keep the fit manageable we proceed as in Ref. [19] and restrict ourselves to the CP-conserving case and set  $\delta_{\text{CP}} \in \{0, \pi\}$ . Consequently the T2K and NO $\nu$ A appearance data (which exhibit substantial dependence on the leptonic CP phase) are not included in the fit. With these data we construct a global  $\chi^2$  function:

$$\chi_{\text{OSC}+Z'}^2(g', M_{Z'} | \vec{\omega}) \quad (3.1)$$

for each  $Z'$  model. In general each model belongs to a family characterized by a set of  $U(1)'$  charges; for each family  $\chi_{\text{OSC}+Z'}^2$  depends on the two variables parametrizing the new interaction,  $g'$  and  $M_{Z'}$ , plus the six oscillation parameters  $\vec{\omega} \equiv (\Delta m_{21}^2, \Delta m_{31}^2, \theta_{12}, \theta_{13}, \theta_{23}, \delta_{\text{CP}})$ .

Following the discussion in Sec. 2, we have performed the analysis in two physically distinctive domains of  $M_{Z'}$ :

- **NSI Domain (DOM=NSI):** In this case, the range of the induced non-standard interactions in both the Sun and the Earth matter is short enough for the four-fermion effective description to hold. As seen in Fig. 1 this happens for  $M_{Z'} \gtrsim 10^{-10}$  eV. In this regime a possible conflict with the cosmological bound on  $\Delta N_{\text{eff}}$  may appear because of the contribution of either the  $Z'$  itself (if lighter than all active neutrinos) or by the extra contribution to the neutrino density produced by the  $Z'$  decay (if heavier than some  $\nu$  mass eigenstate). These bounds can be evaded in two distinct ranges of the  $U(1)'$  interactions:

- $M_{Z'} \gtrsim 5$  MeV for which the contribution to the neutrino energy density due to the decay of the  $Z'$  into neutrinos is sufficiently suppressed by the Boltzmann factor  $\sim \exp(-M_{Z'}/T)$  [41];
- $M_{Z'} \lesssim \mathcal{O}(\text{eV})$  but with very weak coupling  $g' < 10^{-10}$  for which the  $Z'$  is produced through freeze-in. In this regime, even if  $Z'$  could decay to the lightest neutrinos this would happen after neutrino decoupling making the contribution to  $\Delta N_{\text{eff}}$  negligible or at most within the present allowed range [42].
- Long-Range Domain (DOM=LRI): If  $M_{Z'} \lesssim 10^{-13}$  eV interactions in the Earth and Sun matter are long range, and for a given value of  $g'$  and  $M_{Z'}$  the effects in the Earth are suppressed with respect to those in the Sun. As mentioned above, for  $g' < 10^{-10}$  the contribution to  $\Delta N_{\text{eff}}$  is negligible.

Correspondingly we define

$$\chi_{\text{OSC}+Z',\text{DOM}}^2(g', M_{Z'}|\vec{\omega}) \equiv \chi_{\text{OSC}+Z'}^2(g', M_{Z'} \in \text{DOM}|\vec{\omega}) \quad (3.2)$$

In both domains we compare the results of the fit including the new  $U(1)'$  interaction with those obtained in the “standard”  $3\nu$ -mixing scenario, which we will denote as “OSC”, and for which the present global fit yields

$$\chi_{\text{OSC},\text{min}}^2 = 718.5. \quad (3.3)$$

We will classify the models according to the quality of the fit in the presence of the  $U(1)'$  interactions compared with that of OSC by defining

$$\Delta\chi_{\text{LIGHT},\text{DOM}}^2(g', M_{Z'}) \equiv \chi_{\text{OSC}+Z',\text{DOM}}^2(g', M_{Z'}|\vec{\omega})|_{\text{marg,LIGHT}} - \chi_{\text{OSC},\text{min}}^2, \quad (3.4)$$

where by  $|_{\text{marg,LIGHT}}$  we imply that the minimization over the oscillation parameters is done in the LIGHT sector of parameter space. In addition the presence of a viable LMA-D solution can be quantified in terms of

$$\Delta\chi_{\text{DARK},\text{DOM}}^2(g', M_{Z'}) \equiv \chi_{\text{OSC}+Z',\text{DOM}}^2(g', M_{Z'}|\vec{\omega})|_{\text{marg,DARK}} - \chi_{\text{OSC},\text{min}}^2, \quad (3.5)$$

where by  $|_{\text{marg,DARK}}$  we imply that the minimization over the oscillation parameters is done in the DARK sector.

We have surveyed the model space by performing the global oscillation analysis for a grid of  $U(1)'$  interactions characterized by the six couplings  $a_{u,d} \in \{-1, 0, 1\}$  and  $a_e, b_{e,\mu,\tau} \in \{-3, -2, -1, 0, 1, 2, 3\}$ . In this way our survey covers a total of  $\sim 10000$  different sets of  $U(1)'$  charges which can produce effects in matter propagation in neutrino oscillation experiments.

### 3.1 Bounds

We first search for models for which in the LIGHT sector the new interactions lead to a significantly better fit of the oscillation data compared to pure oscillations for some value of  $g'$  and  $M_{Z'}$ . We find that in the NSI (LRI) domain 88% (90%) of the surveyed sets of

Model	$(\Delta\chi^2_{\text{LIGHT,LRI}})_{\min}$	$g' \leq \text{bound}$
$B - 3L_e$	-1.4	$6.6 \times 10^{-27}$
$B - 3L_\mu$	-1.1	$7.0 \times 10^{-27}$
$B - 3L_\tau$	-1.8	$7.3 \times 10^{-27}$
$B - \frac{3}{2}(L_\mu + L_\tau)$	-1.2	$7.2 \times 10^{-27}$
$L_e - L_\mu$	-1.3	$9.7 \times 10^{-27}$
$L_e - L_\tau$	-1.7	$1.0 \times 10^{-26}$
$L_e - \frac{1}{2}(L_\mu + L_\tau)$	-1.4	$9.8 \times 10^{-27}$
Ref. [22]	0	$4.9 \times 10^{-27}$
$L_e + 2L_\mu + 2L_\tau$	0	$6.0 \times 10^{-27}$

**Table 2.** Results for the models with charges in table 1 in the LRI regime. The second column gives minimum  $\Delta\chi^2$  defined w.r.t. the  $3\nu$  oscillation (see Eq. (3.4)). The last column gives the the upper bound for the coupling of asymptotically for ultra light mediators,  $M_{Z'} \lesssim 10^{-15}$  eV

charges lead to a decrease in the  $\chi^2$  of the global analysis when compared to the standard oscillation case. The percentages grow to 100% when restricting to the subclass of anomaly free vector  $Z'$  models with gauging of SM global symmetries with SM plus right-handed neutrinos matter content of Eq. (2.2). However the improvement in the quality of the fit is never statistically significant. As an illustration we show in the second column of tables 2 and 3 the minimum values of  $\Delta\chi^2_{\text{LIGHT,DOM}}$  for  $U(1)'$  interactions characterized by the specific set of charges in table 1. Comparing the two tables we notice that for some of the cases the fit can be slightly better in the LRI domain than in the NSI domain but still below the  $2\sigma$  level.

Quantitatively we find that in the NSI regime none of the surveyed models yields an improvement beyond -1.9 units of  $\chi^2$ . This is the case, for example, of a  $Z'$  coupled to  $B - 3L_e + 2L_\mu + 3L_\tau$ . Generically models in the LRI domain can provide a better fit with a reduction of up to 3.5 units of  $\chi^2$ . For example a model with charge  $L_e + 2L_\mu - 3L_\tau$  and a  $Z'$  with  $M_{Z'} \sim 5 \times 10^{-15}$  eV provides a better fit than standard oscillations by  $(\Delta\chi^2_{\text{LIGHT,LRI}})_{\min} = -3.2$ .

But in summary, our analysis shows that none of the set of charges surveyed in both NSI or LRI domains improved over standard oscillations at the  $2\sigma$  level, this is  $\min_{g', M_{Z'}}(\Delta\chi^2_{\text{LIGHT,DOM}})$  was always larger than -4.<sup>2</sup> Consequently for all models surveyed one can conclude that the analysis of neutrino oscillation experiments show no significant evidence of  $U(1)'$  interactions. Consequently one can exclude models at a certain confidence level – which we have chosen to be 95.45% – by verifying that their global fit is worse than in OSC by the corresponding units of  $\chi^2$  (4 units for 95.45% CL), this is:

$$\Delta\chi^2_{\text{LIGHT,DOM}}(g', M_{Z'}) > 4. \quad (3.6)$$

<sup>2</sup>We notice that before the new results from Super-Kamiokande [35] there were models which could improve the mismatch between the best fit  $\Delta m_{21}^2$  in Solar and KamLAND. For such models, one could find values of  $g'$  and  $M_{Z'}$  for which the fit was better than standard oscillations by more than 4 units of  $\chi^2$ .

Model	$(\Delta\chi^2_{\text{LIGHT,NSI}})_{\min}$	$g' \leq \text{bound} \left( \frac{M_{Z'}}{100 \text{ MeV}} \right)$
$B - 3L_e$	-1.4	$2.0 \times 10^{-4}$
$B - 3L_\mu$	0	$4.6 \times 10^{-5}$
$B - 3L_\tau$	-0.6	$4.7 \times 10^{-5}$
$B - \frac{3}{2}(L_\mu + L_\tau)$	-1.1	$2.2 \times 10^{-4}$
$L_e - L_\mu$	-1.3	$1.2 \times 10^{-4}$
$L_e - L_\tau$	-1.0	$1.2 \times 10^{-4}$
$L_e - \frac{1}{2}(L_\mu + L_\tau)$	-1.3	$3.0 \times 10^{-4}$
Ref. [22]	0	$1.5 \times 10^{-4}$
$L_e + 2L_\mu + 2L_\tau$	-0.1	$1.8 \times 10^{-4}$

**Table 3.** Results for the models with charges in table 1 in the NSI regime. The second column gives minimum  $\Delta\chi^2$  defined w.r.t. the  $3\nu$  oscillation (see Eq. (3.4)). The last column gives the coefficient of the bound on the coupling over the mediator mass in units of 100 MeV.

Let us stress that with the above condition we are not “deriving two-dimensional excluded regions in the parameter space”, but we are instead determining the values of  $g'$  and  $M_{Z'}$  for which the  $U(1)'$  model characterized by such interaction strength and interaction length, gives a fit which is worse than standard oscillations by at least 4 units of  $\chi^2$ . As in the LIGHT sector the standard model is recovered for either  $g' \rightarrow 0$  or  $M_{Z'} \rightarrow \infty$ , the above condition yields also the  $2\sigma$  excluded one-dimensional upper range of interaction coupling  $g'$  for each value of the interaction length (or, correspondingly, the  $2\sigma$  excluded one-dimensional lower range of  $M_{Z'}$  for each value of the interaction coupling), for all models characterized by a given set of charges.

The corresponding excluded ranges for the  $Z'$  coupling and mass for the models with couplings listed in table 1 are shown in Figs. 2 and 3 for  $M_{Z'}$  below 1 eV and in the  $\mathcal{O}(\text{MeV--GeV})$  range, respectively<sup>3</sup> – *i.e.*, below and above the window strongly disfavored by the cosmological bound on  $\Delta N_{\text{eff}}$ . In particular in Fig. 2 we observe the slope change of the oscillation exclusion ranges for masses  $M_{Z'} \sim 10^{-15}\text{--}10^{-13}$  GeV, for which the interaction length is longer than the Earth and Sun radius and the matter potential in the Earth and in the Sun becomes saturated (see Fig. 1). Quantitatively, for the models with charges in table 1 we find that in the LRI domain the analysis of oscillation data yields the upper bound for the coupling of asymptotically ultra light mediators,  $M_{Z'} \lesssim 10^{-15}$  eV which we list in table 2. For the sake of comparison, we also show in Fig. 2 the bounds on these models imposed by gravitational fifth force searches, and by equivalence principle tests. Those are the strongest constraints in the shown range of  $Z'$  mass and coupling. The bounds imposed by gravitational fifth force searches were obtained by rescaling the results shown in Ref. [43] (which, in turn, were recasted from Ref. [44]). Limits from equivalence principle tests are obtained rescaling the results from Ref. [45]. Details of the rescaling of the published bounds applied for the specific models can be found in the Appendix. It is

<sup>3</sup>Tables with the numerical values of the bounds can be provided upon request to the authors.

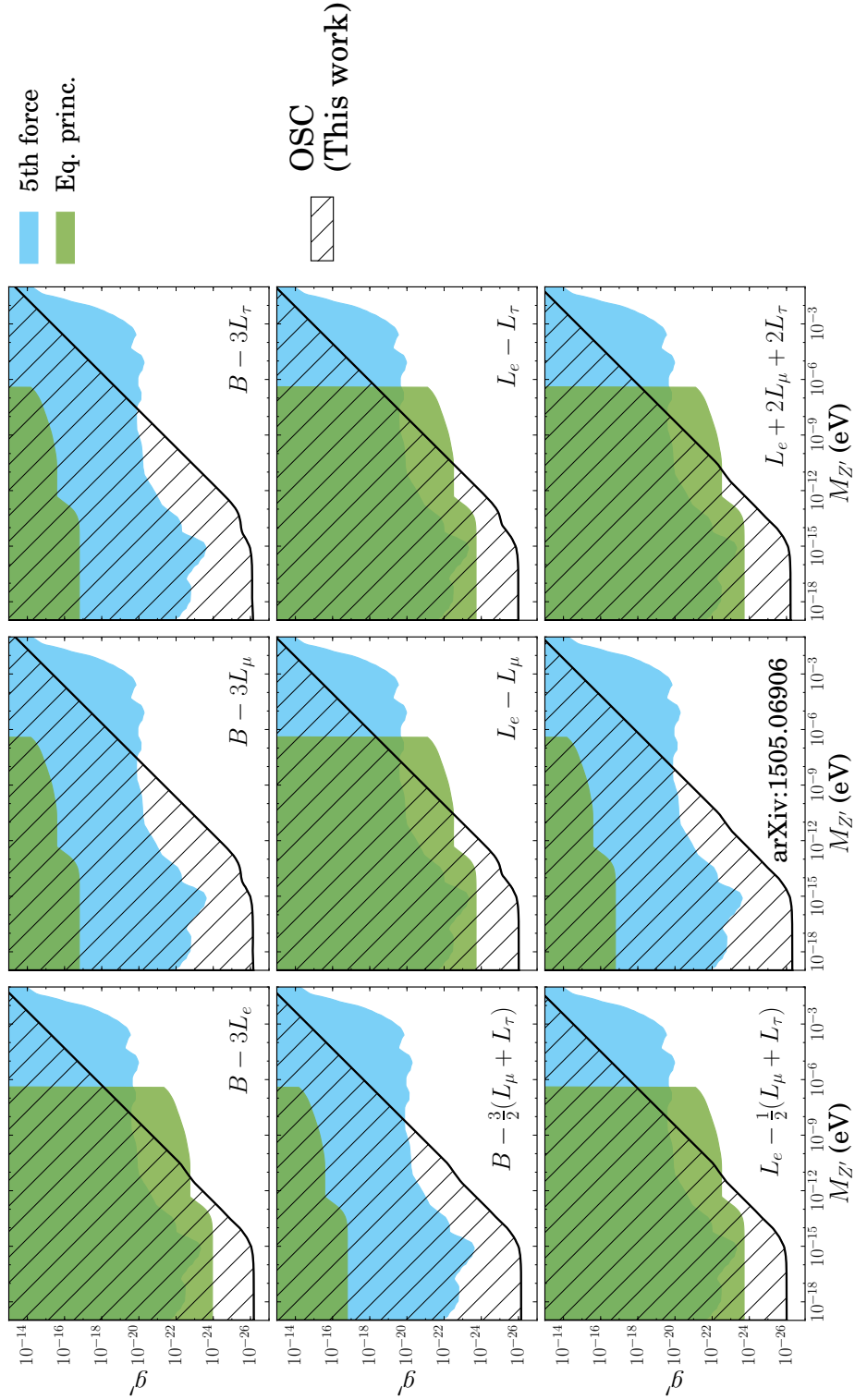


**Figure 2.** Values of  $g'$  and  $M_{Z'} \leq \mathcal{O}(\text{eV})$  for which a  $U(1)'$  model coupled to the charges labeled in each panel gives a worse fit than standard oscillation by  $2\sigma$ , Eq. (3.6) (hatched region). Also show in the figure the bounds on these models imposed by gravitational fifth force searches [43, 44] and by equivalence principle tests [45]. See text for details.

important to notice that these exclusion regions obtained by recasting the boundaries of the published regions may not correspond to the statistical condition we employed, Eq. (3.6). So the comparison has to be taken with a pinch of salt. Still, from the figures we see that, generically, for all models shown the oscillation analysis improves over the existing bounds for  $Z'$  lighter than  $\sim 10^{-8}$  eV or  $\sim 10^{-11}$  eV depending on whether the  $U(1)'$  current involves coupling to electron lepton number.

Conversely the results shown in Fig. 3 for  $M_{Z'}$  in the  $\mathcal{O}(\text{MeV--GeV})$  range correspond to  $U(1)'$  effects in oscillation experiments always in the NSI domain. In this case, the analysis of oscillation data results in a bound on  $g'$  which scales as the inverse of the mediator mass with coefficients which we list in table 3. For the sake of comparison, we also show in Fig. 3 a compilation of the most relevant experimental bounds on these  $U(1)'$  models. These include constraints from electron and proton fixed target experiments, neutrino electron elastic scattering, coherent neutrino nucleus elastic scattering, white dwarf cooling and collider constraints. Appendix A contains all relevant details on the derivation of these bounds.

As seen in Fig. 3 for most models there are values of  $g'$  and  $M_{Z'}$  which are only constrained by the oscillation analysis. This is particularly the case for  $U(1)'$  couplings to  $B - 3L_\mu$ , and the model in Ref. [22] for which the only other bound applying in the shown range of  $g'$  and  $M_{Z'}$  is the one from BaBar. Finally for a  $Z'$  coupled to  $B - 3L_\tau$  we have found no competitive bound from other experiments in the shown window (for bounds from other experiments relevant for larger couplings see for example Refs. [20, 46]).

### 3.2 Models for LMA-D

A subset of models can lead to a best fit in the DARK sector or at least with LMA-D within 4 units of  $\chi^2$  with respect to the standard OSC solution,

$$\Delta\chi_{\text{DARK,DOM}}^2(g', M_{Z'}) < 4. \quad (3.7)$$

As discussed in Sec. 2.2 this can only happen in the NSI domain. In our survey we have found that 4.8% of the set of charges studied can have a best fit in LMA-D, and 5.2% lead to LMA-D verifying Eq. (3.7). However none of these set of charges correspond to the subclass of anomaly free vector  $Z'$  models with gauging of SM global symmetries with SM plus right-handed neutrinos matter content (Eq. (2.2)).

In particular for the first seven set of models in table 1 the LMA-D solutions lies at more than  $5\sigma$  from the standard oscillation fit. On the contrary the models in the last two lines yield a viable LMA-D solution. The first one was proposed in Ref. [22] precisely as a viable model for LMA-D. Indeed in this case we find  $(\Delta\chi_{\text{DARK,NSI}}^2)_{\min} = 1.2$ , which is within 4 units of  $\chi^2$  from the pure oscillation result but the best fit for this model charges still lies within the LIGHT sector. We also show the results for a  $U(1)'$  model coupled to  $L_e + 2L_\mu + 2L_\tau$  for which we find that the best fit is LMA-D with  $(\Delta\chi_{\text{DARK,NSI}}^2)_{\min} = -1.3$ .

In Fig. 4 we plot as black bands the range of coupling and masses for these two set of charges verifying the condition (3.7), together with the compilation of relevant bounds from other experiments.



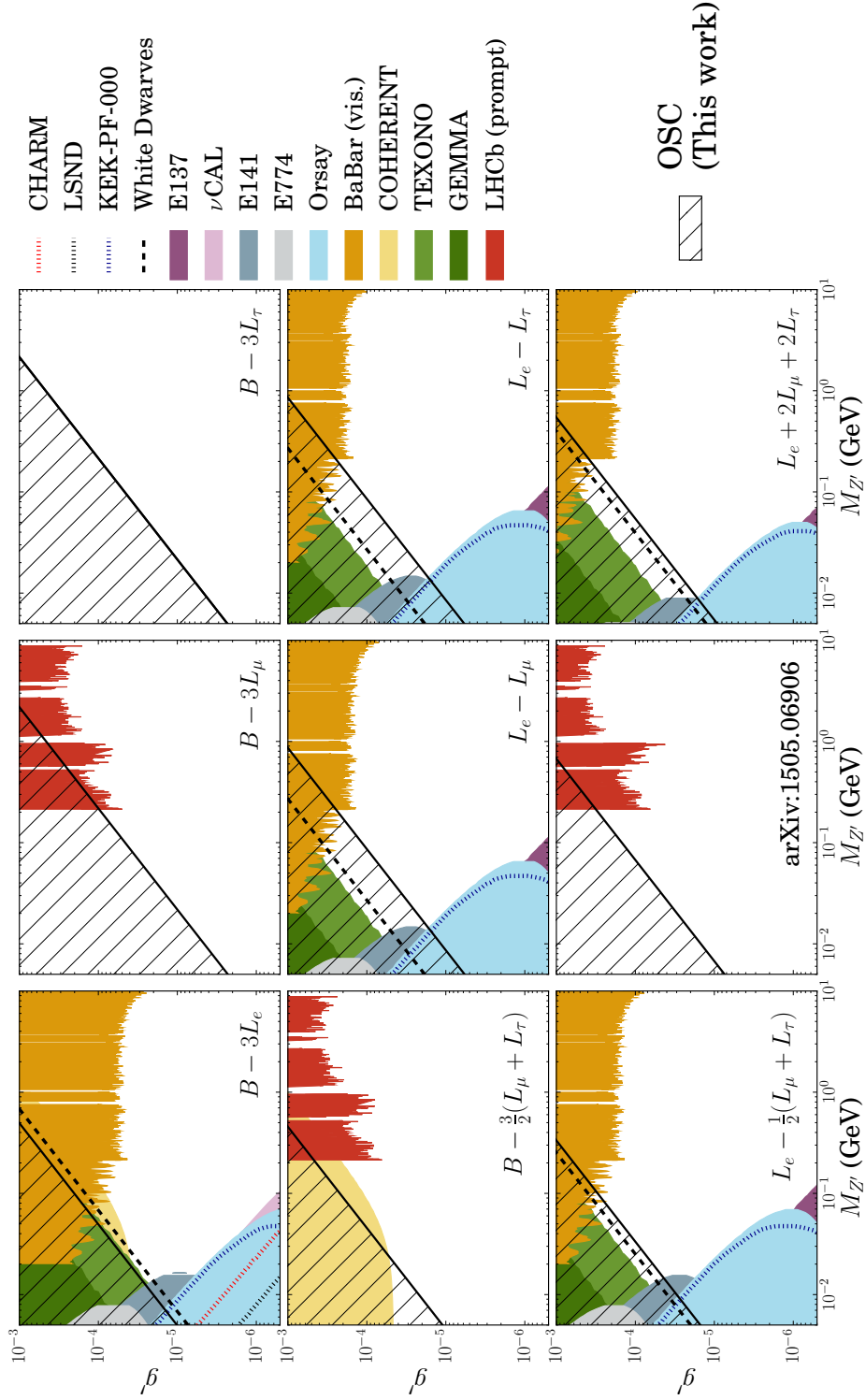


**Figure 3.** Values of  $g'$  and  $5 \text{ MeV} \leq M_{Z'} \leq 10 \text{ GeV}$  for which a  $U(1)'$  model coupled to the charges labeled in each panel gives a worse fit than standard oscillation by  $2\sigma$ , Eq. (3.6) (hatched region). Also show in the figure the bounds on these models imposed by a compilation of experiments as labeled in the figure (see text for details).

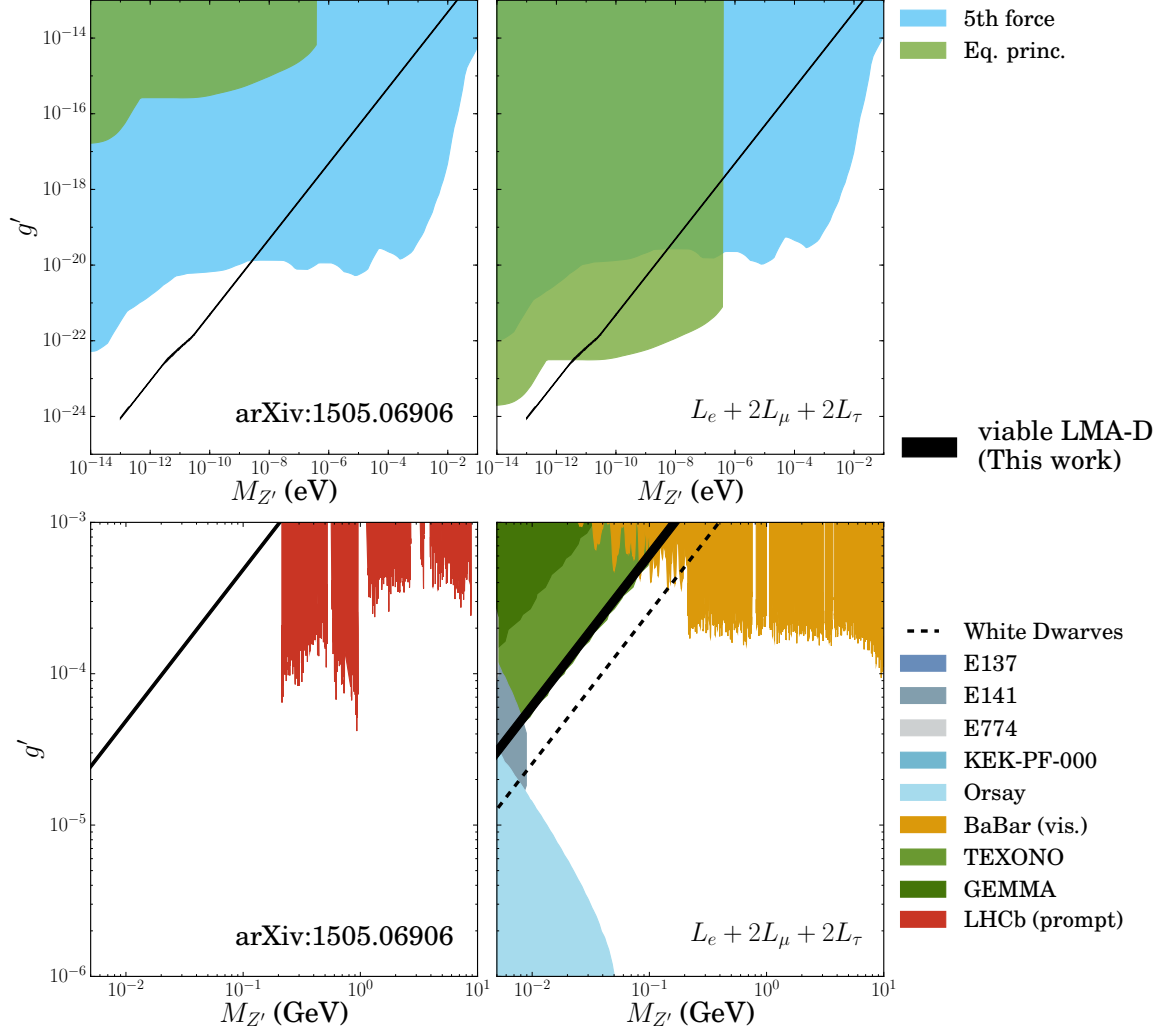


**Figure 4.** Range of  $g'$  and  $M_{Z'}$  for which the global analysis of oscillation data can be consistently described within the LMA-D solution, Eq. (3.7), (black band) for two viable models. Also show in the figure the bounds on these models imposed by a compilation of experiments as labeled in the figure. See text for details.

As seen in the figure, for the model in Ref. [22], there are solutions for the  $Z'$  coupling and mass for which LMA-D is allowed without conflict with bounds from other experiments both for very light mediators as well as for an  $\mathcal{O}(\text{MeV--GeV})$   $Z'$ . More quantitatively for ultra light mediator part of the LMA-D allowed parameter space for the model in Ref. [22] is in conflict with the bounds from fifth force tests which impose the stronger constraints for this model in this regime. But the LMA-D is still a viable solution for

$$10^{-13} \text{ eV} \leq M_{Z'} \leq 2.5 \times 10^{-9} \text{ eV} \quad (3.8)$$

with couplings in a very narrow band and seen in the figure, for example

$$g' = (9.1 \pm 0.2) \times 10^{-25} \quad \text{for} \quad M_{Z'} = 10^{-13} \text{ eV} \quad (3.9)$$

and

$$g' = (1.22 \pm 0.04) \times 10^{-20} \quad \text{for} \quad M_{Z'} = 2.5 \times 10^{-9} \text{ eV}. \quad (3.10)$$

In addition LMA-D is also a viable solution for this model with

$$5 \text{ MeV} \leq M_{Z'} \leq 200 \text{ MeV} \quad \text{with} \quad \frac{g'}{M_{Z'}} = \frac{(4.85 \pm 0.15) \times 10^{-5}}{\text{MeV}}. \quad (3.11)$$

On the contrary, as seen in the figure, the model with charge  $L_e + 2L_\mu + 2L_\tau$  can only provide a viable LMA-D solution without conflict with bounds from other experiments for and ultra light mediator with  $M_{Z'} \lesssim 5 \times 10^{-12} \text{ eV}$ .

## 4 Conclusions

In this work we have performed dedicated global analysis of oscillation data in the framework of lepton flavor dependent  $U(1)'$  interactions which affect the neutrino evolution in matter. The analysis is performed for interaction lengths ranging from larger than the Sun radius (covering what we label as LRI domain) to effective contact neutrino interactions (NSI domain). We survey  $\sim 10000$  set of models characterized by the charges of the first generation charged fermions and the three flavor neutrinos. We find that

- In the LIGHT sector of the oscillation parameter space the introduction of new interactions does not lead to a significantly better fit of the oscillation data compared to standard oscillations, irrespective of the  $U(1)'$  coupling in either NSI or LRI domains. Thus for all cases the analysis of oscillation data in the LIGHT sector results in excluded ranges of  $g'$  and  $M_{Z'}$ .
- The excluded ranges for the  $Z'$  coupling and mass for the models with couplings listed in table 1 are shown in Figs. 2 and 3 for  $M_{Z'}$  below 1 eV and in the  $\mathcal{O}(\text{MeV--GeV})$  range, respectively – *i.e.*, below and above the window strongly disfavored by the cosmological bound on  $\Delta N_{\text{eff}}$ .
- In the regime of ultra-light mediators, for all models shown, the oscillation analysis improves over the bounds from tests of fifth forces and of violation of equivalence principle and for  $Z'$  lighter than  $\sim 10^{-8} \text{ eV}$  or  $\sim 10^{-11} \text{ eV}$  depending on whether the  $U(1)'$  current involves coupling to electron lepton number.

- For mediators in the  $\mathcal{O}(\text{MeV--GeV})$  range we list in table 3 the derived constraints on  $g'$  versus  $M_{Z'}$ . We find that for most of the considered models there are values of  $g'$  and  $M_{Z'}$  for which the oscillation analysis provides constraints extending beyond those from other experiments.
- In what respects to LMA-D we find that it cannot be realized in the LRI domain. In the NSI domain we have found that 4.8% of the set of charges studied can have a best fit in LMA-D, and 5.2% lead to LMA-D as a valid solution within 4 units of  $\Delta\chi^2$  of standard oscillations. None of these set of charges correspond to an anomaly free model based on gauging SM global symmetries with SM plus right-handed neutrinos matter content (Eq. (2.2)). So, generically,  $Z'$  models for LMA-D with gauged SM global symmetries require additional states for anomaly cancellation.

## Acknowledgement

We want to thank Renata Zukanovich for discussions and her participation in the early stages of this work. The authors also acknowledge use of the HPC facilities at the IFT (Hydra cluster). This work was supported by the spanish grants FPA2016-76005-C2-1-P, FPA2016-78645-P, PID2019-105614GB-C21 and PID2019-110058GB-C21, by USA-NSF grant PHY-1915093, by AGAUR (Generalitat de Catalunya) grant 2017-SGR-929. The authors acknowledge the support of the Spanish Agencia Estatal de Investigación through the grant “IFT Centro de Excelencia Severo Ochoa SEV-2016-0597”.

## A Bounds from non-oscillation experiments

Here we summarize the main details of the bounds shown by the colored regions in Figs. 2 and 3, as well as the procedure used to rescale them for the different models shown in each panel.

### Bounds from searches for gravitational fifth forces

Generically gravitational fifth force experiments look for deviation from the standard Newton potential ( $\propto 1/r$ ) between two objects.

We have taken the results from Ref. [43] (which, in turn, were recasted from Fig. 10 in Ref. [44]) where they present the constraints on the coupling  $\alpha_5$  versus the interaction length  $\lambda$  (or, equivalently, versus  $m_5 = \frac{1}{\lambda}$ ) defined as the constant entering the potential of the fifth force

$$V_5(r) = \alpha_5 \mathcal{N}_1 \mathcal{N}_2 \frac{e^{-r/\lambda}}{r} \quad (\text{A.1})$$

where  $\mathcal{N}_{1,2}$  is the total charge of each object, which they take as the total number of baryons.

In particular from Fig. 3 in [43] we read their boundary curve

$$\left( \frac{\alpha_5^{\max}}{\alpha_{em}}, m_5 \right), \quad (\text{A.2})$$

where  $\alpha_{em}$  is the SM fine structure constant. In order to rescale it to the different  $U(1)'$  models we notice that the corresponding potential for the  $U(1)'$  interaction for the same objects is

$$V'(r) = C_1 C_2 \frac{g'^2}{4\pi} \frac{e^{-r/\lambda'}}{r}, \quad (\text{A.3})$$

where  $C_i$  is the total  $Z'$  charge of object  $i$  and  $\lambda'$  is the  $U(1)'$  interaction length

$$\lambda' = \frac{1}{M_{Z'}}, \quad C_i \equiv \frac{\mathcal{N}_i}{A_i} c_i \equiv \frac{\mathcal{N}_i}{A_i} [Z_i(a_e + 2a_u + a_d) + (A_i - Z_i)(a_u + 2a_d)], \quad (\text{A.4})$$

where  $Z_i$  and  $A_i$  are the atomic number and mass number of the material of which the object  $i$  is made, so  $c_i$  is the charge under  $Z'$  for each atom of the material. Assuming that the number of protons and neutrons in the material are not very different (that is,  $A_i/Z_i \sim 2$ ), we get

$$V'(r) = V_5(r) \times \frac{g'^2}{4\pi\alpha_5} \frac{(a_e + 3a_u + 3a_d)^2}{4} \quad (\text{A.5})$$

with  $m_5 = M_{Z'}$ . So the boundary in the  $g'$  vs  $M_{Z'}$  plane will be

$$(g'_{\max}, M_{Z'}) = \left( \frac{2}{a_e + 3a_u + 3a_d} \sqrt{4\pi\alpha_{em}} \times \sqrt{\frac{\alpha_5^{\max}}{\alpha_{em}}}, m_5 \right). \quad (\text{A.6})$$

### **Bounds from searches for violation of the equivalence principle**

Similarly as in the case of fifth force searches, this bound comes from precise measurements of the gravitational potential between two objects. However, in this case one tests the differences of the potential for the same total mass of two different test materials, using a pendulum which is attracted by the same mass. The bounds are taken from Ref. [45], where they define the potential due to the new force as:

$$V_G(r) = \alpha G \frac{m_t m_s}{r} \hat{\mathcal{N}}_t \hat{\mathcal{N}}_s e^{-r/\lambda}. \quad (\text{A.7})$$

where  $G$  is the gravitational constant,  $\hat{\mathcal{N}}_i$  refers to the new interaction charge per mass unit, and the subindices  $t$  and  $s$  stand for test (or pendulum) and source masses, respectively. In Ref. [45] they assume that the new interaction couples to the number of baryons. Thus, they use beryllium and titanium as test materials, chosen to maximize the difference in baryon number per unit mass. To be specific, we use  $\hat{\mathcal{N}}_{\text{Be}} = 0.99868$  and  $\hat{\mathcal{N}}_{\text{Ti}} = 1.001077$ , as in Ref. [45].

Noting that the total potential will be the sum of the standard gravitational potential plus the contribution from the new interaction, the authors of Ref. [45] put a bound on

$$\eta = 2 \frac{V_{\text{Be}} - V_{\text{Ti}}}{V_{\text{Be}} + V_{\text{Ti}}} \sim \frac{\Delta V_G(r)}{\frac{G m_s m_t}{r}} = \alpha (\hat{\mathcal{N}}_{\text{Ti}} - \hat{\mathcal{N}}_{\text{Be}}) \hat{\mathcal{N}}_s e^{-r/\lambda} \quad (\text{A.8})$$

which is used to set a constraint on  $\alpha$  as a function of  $\lambda$ ,

$$(\alpha^{\max}, \lambda). \quad (\text{A.9})$$

This can be used to set a bound on  $\Delta V'(r)$  for a general model, noting that

$$\begin{aligned}
\Delta V'(r) &= \frac{g'^2}{4\pi} \frac{e^{-rM_{Z'}}}{r} C_s (C_{\text{Be}} - C_{\text{Ti}}) \\
&= \Delta V_G(r) \times \frac{g'^2/4\pi}{\alpha G \cdot u^2} \times \frac{c_{\text{Ti}}/A_{\text{Ti}} - c_{\text{Be}}/A_{\text{Be}}}{\hat{\mathcal{N}}_{\text{Ti}} - \hat{\mathcal{N}}_{\text{Be}}} \times \frac{c_s/A_s}{\hat{\mathcal{N}}_s} \\
&\simeq \Delta V_G(r) \times \frac{g'^2/4\pi}{\alpha G \cdot u^2} \times \frac{(a_e + a_u - a_d)(a_e + 3a_u + 3a_d)}{144(\hat{\mathcal{N}}_{\text{Ti}} - \hat{\mathcal{N}}_{\text{Be}})}
\end{aligned} \tag{A.10}$$

where  $u$  stands for the atomic mass unit in GeV ( $u \simeq 0.931$  GeV), and in the last line we have approximated for the source material  $A/Z \simeq 2$  and  $\hat{\mathcal{N}}_s \simeq 1$ . So the boundary in the  $g'$  vs  $M_{Z'}$  plane will be

$$(g'_{\text{max}}, M_{Z'}) = \left( \sqrt{\frac{144(\hat{\mathcal{N}}_{\text{Ti}} - \hat{\mathcal{N}}_{\text{Be}})}{(a_e + 3a_u + 3a_d)(a_e + a_u - a_d)}} 4\pi G u^2 \times \sqrt{\alpha^{\text{max}}}, \frac{1}{\lambda} \right) \tag{A.11}$$

### Bounds from white-dwarf cooling

We based the bounds shown in Figs. 3 and 4 on the study presented in Ref. [47]. There, upper bounds on new interactions are imposed on the basis that the energy losses from plasmon decays into particles that escape the star is not larger than the energy losses due to neutrino emission in the SM.

In the  $U(1)'$  scenarios here considered the minimum new contribution is due to  $Z'$  mediated decays into neutrinos

$$\Gamma_{\text{plasmon} \rightarrow \nu \bar{\nu}, Z'}^s \lesssim \Gamma_{\text{plasmon} \rightarrow \nu \bar{\nu}, \text{SM}}^s = \frac{C_{e,V}^2 G_F^2}{48\pi^2 \alpha_{em}} \frac{Z_s \pi_s^3}{\omega_s} \tag{A.12}$$

where  $C_{e,V}$  is the vector coupling to the electron current in the SM,  $Z_s$  is the plasmon wavefunction renormalization and  $\pi_s$  is the effective plasmon mass which enters in the dispersion relation  $\omega_s^2 - k^2 = \pi_s(\omega_s, k)$ . Here,  $s = T, L$  refers to the plasmon polarization (transverse or longitudinal).

Under the assumption that the mass of the  $Z'$  is much larger than the frequency of the plasmon we can write its rate into neutrinos of a given flavor  $\beta$  due to the new interactions as

$$\Gamma_{\text{plasmon} \rightarrow \nu_\beta \bar{\nu}_\beta, Z'}^s = \frac{1}{3} \frac{g'^4}{M_{Z'}^4} \frac{(a_e b_\beta)^2}{48\pi^2 \alpha_{em}} \frac{Z_s \pi_s^3}{\omega_s} \tag{A.13}$$

And the upper bound obtained in Ref. [47] translates into:

$$\sqrt{\sum_\beta \frac{(a_e b_\beta)^2}{3}} \cdot \frac{g'^2}{M_{Z'}^2} \leq C_{e,V} G_F = 1.12 \times 10^{-5} \text{ GeV}^{-2}. \tag{A.14}$$

### Bounds from coherent neutrino-nucleus scattering

We have performed our own reanalysis of coherent neutrino-nucleus scattering data using the time and energy information from COHERENT experiment [48, 49] on CsI based on

our recent analysis in Ref. [50] performed for NSI with a variety of nuclear form factors, quenching factors and parametrization of the background. In particular the results shown in Fig. 3 correspond to the analysis performed using the quenching factor obtained with the fit to the calibration data of the Duke (TUNL) group [48] together with our data driven reevaluation of the steady-state background (see Ref. [50] for details).

Model predictions are obtained exactly as in [50], but replacing the cross section for coherent scattering in the presence of NSI with that induced by the  $Z'$ . In particular if we define

$$\varepsilon'(Q^2, g', M_{Z'}) \equiv \frac{1}{\sqrt{2}G_F} \frac{g'^2}{M_{Z'}^2 + Q^2} \quad (\text{A.15})$$

one can use the same cross section expression for NSI simply replacing:

$$\varepsilon_{\alpha\beta}^{q,V} \rightarrow \delta_{\alpha\beta} a_q b_\alpha \varepsilon'(Q^2, g_X, M_{Z'}) \quad (\text{A.16})$$

where  $Q^2 = 2MT$  is the momentum transfer. In this case, the differential cross section for coherent scattering of a neutrino with flavor  $\alpha$  reads:

$$\frac{d\sigma_\alpha}{dT} = \frac{G_F^2}{2\pi} W_\alpha^2(Q^2, g_X, M_{Z'}) F^2(Q^2) M \left( 2 - \frac{MT}{E_\nu^2} \right) \quad (\text{A.17})$$

where  $M$  is the mass of the nucleus,  $T$  is the nuclear recoil energy, and  $E_\nu$  is the incident neutrino energy. We have defined a modified weak charge for the nucleus as:

$$W_\alpha(Q^2, g_X, M_{Z'}) = Z[g_p^V + (2a_u + a_d) b_\alpha \varepsilon'(Q^2, g_X, M_{Z'})] + N[g_n^V + (a_u + 2a_d) b_\alpha \varepsilon'(Q^2, g_X, M_{Z'})]. \quad (\text{A.18})$$

Thus, unlike in the case of NSI, the weak charge now depends on the momentum transferred in the process.

The construction of  $\chi_{\text{COH}}^2(g', M_{Z'})$  is totally analogous to that of  $\chi_{\text{COH}}^2(\vec{\varepsilon})$  in Ref. [50]. In consistency with the condition impose when deriving the oscillation bounds the COHERENT regions shown in Fig. 3 corresponds to the  $Z'$  coupling and mass for which the fit to COHERENT data is worse than the one obtained in the SM by 4 units:

$$\chi_{\text{COH}}^2(g', M_{Z'}) - \chi_{\text{COH,SM}}^2 > 4. \quad (\text{A.19})$$

### **Bounds from measurements of neutrino scattering on electrons**

For neutrino-electron scattering experiments TEXONO and GEMMA we performed our own analysis following the procedure in Ref. [51] which explicitly studied the bounds imposed by those experiments in some  $Z'$  models and provide all the relevant cross section expressions.

For TEXONO we use the data from Fig. 16 in Ref. [52]. This corresponds to 29882 (7369) kg-day of fiducial mass exposure during Reactor ON (OFF), respectively. The adopted analysis window is 3–8 MeV, spread out uniformly over  $N_{\text{bin}} = 10$  energy bins. An overall normalization constant has been manually set to reproduce the SM prediction shown in Fig 16 in [52]. Cross section has been implemented following [51]. With this we get  $\chi_{\text{SM,TEXONO}}^2 = 15.87$ .

For GEMMA we take data from Fig. 8 in Ref. [53] and consider both phase I and phase II data so we define  $\chi^2_{\text{GEMMA,TOT}} = \chi^2_{\text{GEMMA,I}} + \chi^2_{\text{GEMMA,II}}$ . This corresponds to about 12000 ON-hours and 3000 OFF-hours of active time. Data was taken for a detector mass of 1.5 kg. The energy window used is  $0.015 \text{ MeV} \leq E_\nu \leq 8.0 \text{ MeV}$ . With this procedure we get  $\chi^2_{\text{SM,GEMMA}} = 154.97$ .

For both TEXONO and GEMMA we draw the contours with the equivalent condition used for the oscillation analysis so for a given set of model charges the contours are defined by  $\chi^2(g', M_{Z'}) - \chi^2_{\text{SM}} = 4$ .

### Other constraints: fixed target experiments and colliders

As mentioned in the text, the bounds from fixed target experiments and colliders are taken directly from the literature. In particular, we consider the following set of bounds:

- Electron beam dump experiments: we take these from the compilation in Ref. [54], which were obtained using data from E137 [55], E141 [56], E774 [57], Orsay [58], and KEK-PF-000 [59].
- Proton beam dump experiments: for LSND we use the results obtained in Ref. [60] which used data from Ref. [61] (see also Ref. [62]); for CHARM [63] we use the limit derived in Ref. [64]; finally, for  $\nu$ -Cal [65] we use the limit derived in Ref. [66] (see also Ref. [67] for a similar analysis).
- We also consider constraints from  $Z'$  production in  $e^+e^-$  collisions in BaBar both in visible [68] and invisible [69] final states, as well as constraints from LHCb for  $U(1)'$  decaying into  $\mu^+\mu^-$ , the most relevant ones being from prompt decay searches [70, 71].

All the bounds mentioned above were obtained for a dark photon coupled to the SM fermions via kinetic mixing. In order to recast these to bounds on the different  $U(1)'$  models considered we have used the `darkcast` software [72], which takes into account the difference in production branching ratio and lifetime of the new boson, as well as its decay into a given final state.

### References

- [1] B. Pontecorvo, *Neutrino Experiments and the Problem of Conservation of Leptonic Charge*, *Sov. Phys. JETP* **26** (1968) 984.
- [2] V.N. Gribov and B. Pontecorvo, *Neutrino astronomy and lepton charge*, *Phys. Lett.* **B28** (1969) 493.
- [3] M.C. Gonzalez-Garcia and M. Maltoni, *Phenomenology with Massive Neutrinos*, *Phys. Rept.* **460** (2008) 1 [0704.1800].
- [4] L. Wolfenstein, *Neutrino Oscillations in Matter*, *Phys. Rev.* **D17** (1978) 2369.
- [5] S.P. Mikheev and A.Y. Smirnov, *Resonance enhancement of oscillations in matter and solar neutrino spectroscopy*, *Sov. J. Nucl. Phys.* **42** (1985) 913.
- [6] J.W.F. Valle, *Resonant Oscillations of Massless Neutrinos in Matter*, *Phys. Lett.* **B199** (1987) 432.



- [7] M.M. Guzzo, A. Masiero and S.T. Petcov, *On the MSW effect with massless neutrinos and no mixing in the vacuum*, *Phys. Lett. B* **260** (1991) 154.
- [8] T. Ohlsson, *Status of non-standard neutrino interactions*, *Rept. Prog. Phys.* **76** (2013) 044201 [[1209.2710](#)].
- [9] O.G. Miranda and H. Nunokawa, *Non standard neutrino interactions: current status and future prospects*, *New J. Phys.* **17** (2015) 095002 [[1505.06254](#)].
- [10] Y. Farzan and M. Tortola, *Neutrino oscillations and Non-Standard Interactions*, *Front. in Phys.* **6** (2018) 10 [[1710.09360](#)].
- [11] P.S. Bhupal Dev et al., *Neutrino Non-Standard Interactions: A Status Report*, in *NTN Workshop on Neutrino Non-Standard Interactions St Louis, MO, USA, May 29-31, 2019*, 2019, <http://lss.fnal.gov/archive/2019/conf/fermilab-conf-19-299-t.pdf> [[1907.00991](#)].
- [12] M.C. Gonzalez-Garcia, P.C. de Holanda, E. Masso and R. Zukanovich Funchal, *Probing long-range leptonic forces with solar and reactor neutrinos*, *JCAP* **0701** (2007) 005 [[hep-ph/0609094](#)].
- [13] J. Grifols and E. Masso, *Neutrino oscillations in the sun probe long range leptonic forces*, *Phys. Lett. B* **579** (2004) 123 [[hep-ph/0311141](#)].
- [14] A.S. Joshipura and S. Mohanty, *Constraints on flavor dependent long range forces from atmospheric neutrino observations at super-Kamiokande*, *Phys. Lett. B* **584** (2004) 103 [[hep-ph/0310210](#)].
- [15] H. Davoudiasl, H.-S. Lee and W.J. Marciano, *Long-Range Lepton Flavor Interactions and Neutrino Oscillations*, *Phys. Rev. D* **84** (2011) 013009 [[1102.5352](#)].
- [16] M.B. Wise and Y. Zhang, *Lepton Flavorful Fifth Force and Depth-dependent Neutrino Matter Interactions*, *JHEP* **06** (2018) 053 [[1803.00591](#)].
- [17] M.C. Gonzalez-Garcia, M. Maltoni and J. Salvado, *Testing matter effects in propagation of atmospheric and long-baseline neutrinos*, *JHEP* **05** (2011) 075 [[1103.4365](#)].
- [18] M.C. Gonzalez-Garcia and M. Maltoni, *Determination of matter potential from global analysis of neutrino oscillation data*, *JHEP* **09** (2013) 152 [[1307.3092](#)].
- [19] I. Esteban, M.C. Gonzalez-Garcia, M. Maltoni, I. Martinez-Soler and J. Salvado, *Updated Constraints on Non-Standard Interactions from Global Analysis of Oscillation Data*, *JHEP* **08** (2018) 180 [[1805.04530](#)].
- [20] J. Heeck, M. Lindner, W. Rodejohann and S. Vogl, *Non-Standard Neutrino Interactions and Neutral Gauge Bosons*, *SciPost Phys.* **6** (2019) 038 [[1812.04067](#)].
- [21] O.G. Miranda, M.A. Tortola and J.W.F. Valle, *Are solar neutrino oscillations robust?*, *JHEP* **10** (2006) 008 [[hep-ph/0406280](#)].
- [22] Y. Farzan, *A model for large non-standard interactions of neutrinos leading to the LMA-Dark solution*, *Phys. Lett. B* **748** (2015) 311 [[1505.06906](#)].
- [23] Y. Farzan and I.M. Shoemaker, *Lepton Flavor Violating Non-Standard Interactions via Light Mediators*, *JHEP* **07** (2016) 033 [[1512.09147](#)].
- [24] K.S. Babu, A. Friedland, P.A.N. Machado and I. Mocioiu, *Flavor Gauge Models Below the Fermi Scale*, [1705.01822](#).

- [25] P.B. Denton, Y. Farzan and I.M. Shoemaker, *Testing large non-standard neutrino interactions with arbitrary mediator mass after COHERENT data*, *JHEP* **07** (2018) 037 [[1804.03660](#)].
- [26] B.C. Allanach, J. Davighi and S. Melville, *An Anomaly-free Atlas: charting the space of flavour-dependent gauged  $U(1)$  extensions of the Standard Model*, *JHEP* **02** (2019) 082 [[1812.04602](#)].
- [27] Z. Maki, M. Nakagawa and S. Sakata, *Remarks on the unified model of elementary particles*, *Prog. Theor. Phys.* **28** (1962) 870.
- [28] M. Kobayashi and T. Maskawa, *CP Violation in the Renormalizable Theory of Weak Interaction*, *Prog. Theor. Phys.* **49** (1973) 652.
- [29] P. Coloma and T. Schwetz, *Generalized mass ordering degeneracy in neutrino oscillation experiments*, *Phys. Rev.* **D94** (2016) 055005 [[1604.05772](#)].
- [30] A. Dziewonski and D. Anderson, *Preliminary reference earth model*, *Phys. Earth Planet. Interiors* **25** (1981) 297.
- [31] T.-K. Kuo and J.T. Pantaleone, *THE SOLAR NEUTRINO PROBLEM AND THREE NEUTRINO OSCILLATIONS*, *Phys. Rev. Lett.* **57** (1986) 1805.
- [32] M. Guzzo, H. Nunokawa, P. de Holanda and O. Peres, *On the massless 'just-so' solution to the solar neutrino problem*, *Phys. Rev.* **D64** (2001) 097301 [[hep-ph/0012089](#)].
- [33] P. Bakhti and Y. Farzan, *Shedding Light on Lma-Dark Solar Neutrino Solution by Medium Baseline Reactor Experiments: Juno and Reno-50*, *JHEP* **07** (2014) 064 [[1403.0744](#)].
- [34] I. Esteban, M. Gonzalez-Garcia, A. Hernandez-Cabezudo, M. Maltoni and T. Schwetz, *Global analysis of three-flavour neutrino oscillations: synergies and tensions in the determination of  $\theta_{23}$ ,  $\delta_{CP}$ , and the mass ordering*, *JHEP* **01** (2019) 106 [[1811.05487](#)].
- [35] Y. Nakajima, “SuperKamiokande.”
- [36] I. Esteban, M. Gonzalez-Garcia, M. Maltoni, T. Schwetz and A. Zhou, *The fate of hints: updated global analysis of three-flavor neutrino oscillations*, [2007.14792](#).
- [37] J. Yoo, “RENO.”
- [38] T. Bezerra, “New Results from the Double Chooz Experiment.”
- [39] P. Dunne, “Latest Neutrino Oscillation Results from T2K.”
- [40] A. Himmel, “New Oscillation Results from the NOvA Experiment.”
- [41] A. Kamada and H.-B. Yu, *Coherent Propagation of PeV Neutrinos and the Dip in the Neutrino Spectrum at IceCube*, *Phys. Rev.* **D92** (2015) 113004 [[1504.00711](#)].
- [42] M. Escudero, D. Hooper, G. Krnjaic and M. Pierre, *Cosmology with a Very Light  $L_\mu$ - $L_\tau$  Gauge Boson*, *JHEP* **03** (2019) 071 [[1901.02010](#)].
- [43] E.J. Salumbides, W. Ubachs and V.I. Korobov, *Bounds on fifth forces at the sub-Angstrom length scale*, *J. Molec. Spectrosc.* **300** (2014) 65 [[1308.1711](#)].
- [44] E. Adelberger, J. Gundlach, B. Heckel, S. Hoedl and S. Schlamminger, *Torsion balance experiments: A low-energy frontier of particle physics*, *Prog. Part. Nucl. Phys.* **62** (2009) 102.
- [45] S. Schlamminger, K.Y. Choi, T.A. Wagner, J.H. Gundlach and E.G. Adelberger, *Test of the equivalence principle using a rotating torsion balance*, *Phys. Rev. Lett.* **100** (2008) 041101 [[0712.0607](#)].

- [46] Y. Farzan and J. Heeck, *Neutrinophilic nonstandard interactions*, *Phys. Rev.* **D94** (2016) 053010 [[1607.07616](#)].
- [47] H.K. Dreiner, J.-F. Fortin, J. Isern and L. Ubaldi, *White Dwarfs constrain Dark Forces*, *Phys. Rev.* **D88** (2013) 043517 [[1303.7232](#)].
- [48] COHERENT collaboration, *Observation of Coherent Elastic Neutrino-Nucleus Scattering*, *Science* **357** (2017) 1123 [[1708.01294](#)].
- [49] COHERENT collaboration, *COHERENT Collaboration data release from the first observation of coherent elastic neutrino-nucleus scattering*, [1804.09459](#).
- [50] P. Coloma, I. Esteban, M. Gonzalez-Garcia and M. Maltoni, *Improved global fit to Non-Standard neutrino Interactions using COHERENT energy and timing data*, *JHEP* **02** (2020) 023 [[1911.09109](#)].
- [51] M. Lindner, F.S. Queiroz, W. Rodejohann and X.-J. Xu, *Neutrino-electron scattering: general constraints on  $Z'$  and dark photon models*, *JHEP* **05** (2018) 098 [[1803.00060](#)].
- [52] TEXONO collaboration, *Measurement of  $\text{Nu}(e)\text{-bar}$  -Electron Scattering Cross-Section with a CsI(Tl) Scintillating Crystal Array at the Kuo-Sheng Nuclear Power Reactor*, *Phys. Rev. D* **81** (2010) 072001 [[0911.1597](#)].
- [53] A. Beda, V. Brudanin, V. Egorov, D. Medvedev, V. Pogosov, M. Shirchenko et al., *Upper limit on the neutrino magnetic moment from three years of data from the GEMMA spectrometer*, [1005.2736](#).
- [54] S. Andreas, C. Niebuhr and A. Ringwald, *New Limits on Hidden Photons from Past Electron Beam Dumps*, *Phys. Rev.* **D86** (2012) 095019 [[1209.6083](#)].
- [55] J.D. Bjorken, S. Ecklund, W.R. Nelson, A. Abashian, C. Church, B. Lu et al., *Search for Neutral Metastable Penetrating Particles Produced in the SLAC Beam Dump*, *Phys. Rev.* **D38** (1988) 3375.
- [56] E.M. Riordan et al., *A Search for Short Lived Axions in an Electron Beam Dump Experiment*, *Phys. Rev. Lett.* **59** (1987) 755.
- [57] A. Bross, M. Crisler, S.H. Pordes, J. Volk, S. Errede and J. Wrbanek, *A Search for Shortlived Particles Produced in an Electron Beam Dump*, *Phys. Rev. Lett.* **67** (1991) 2942.
- [58] M. Davier and H. Nguyen Ngoc, *An Unambiguous Search for a Light Higgs Boson*, *Phys. Lett.* **B229** (1989) 150.
- [59] A. Konaka et al., *Search for Neutral Particles in Electron Beam Dump Experiment*, *Phys. Rev. Lett.* **57** (1986) 659.
- [60] R. Essig, R. Harnik, J. Kaplan and N. Toro, *Discovering New Light States at Neutrino Experiments*, *Phys. Rev.* **D82** (2010) 113008 [[1008.0636](#)].
- [61] LSND collaboration, *Search for  $\pi^0 \rightarrow \nu(\mu) \text{ anti-}\nu(\mu)$  decay in LSND*, *Phys. Rev. Lett.* **92** (2004) 091801 [[hep-ex/0310060](#)].
- [62] B. Batell, M. Pospelov and A. Ritz, *Exploring Portals to a Hidden Sector Through Fixed Targets*, *Phys. Rev.* **D80** (2009) 095024 [[0906.5614](#)].
- [63] CHARM collaboration, *Search for Axion Like Particle Production in 400-GeV Proton - Copper Interactions*, *Phys. Lett.* **157B** (1985) 458.
- [64] S.N. Gninenko, *Constraints on sub-GeV hidden sector gauge bosons from a search for heavy neutrino decays*, *Phys. Lett.* **B713** (2012) 244 [[1204.3583](#)].

- [65] J. Blumlein et al., *Limits on neutral light scalar and pseudoscalar particles in a proton beam dump experiment*, *Z. Phys. C* **51** (1991) 341.
- [66] Y.-D. Tsai, P. deNiverville and M.X. Liu, *The High-Energy Frontier of the Intensity Frontier: Closing the Dark Photon, Inelastic Dark Matter, and Muon  $g-2$  Windows*, [1908.07525](#).
- [67] J. Blumlein and J. Brunner, *New Exclusion Limits for Dark Gauge Forces from Beam-Dump Data*, *Phys. Lett. B* **701** (2011) 155 [[1104.2747](#)].
- [68] BABAR collaboration, *Search for a Dark Photon in  $e^+e^-$  Collisions at BaBar*, *Phys. Rev. Lett.* **113** (2014) 201801 [[1406.2980](#)].
- [69] BABAR collaboration, *Search for Invisible Decays of a Dark Photon Produced in  $e^+e^-$  Collisions at BaBar*, *Phys. Rev. Lett.* **119** (2017) 131804 [[1702.03327](#)].
- [70] LHCb collaboration, *Search for  $A' \rightarrow \mu^+\mu^-$  Decays*, *Phys. Rev. Lett.* **124** (2020) 041801 [[1910.06926](#)].
- [71] P. Ilten, Y. Soreq, J. Thaler, M. Williams and W. Xue, *Proposed Inclusive Dark Photon Search at LHCb*, *Phys. Rev. Lett.* **116** (2016) 251803 [[1603.08926](#)].
- [72] P. Ilten, Y. Soreq, M. Williams and W. Xue, *Serendipity in dark photon searches*, *JHEP* **06** (2018) 004 [[1801.04847](#)].